

Tafel Analysis Predicts Cooperative Redox Enhancement Effects in Thermocatalytic Alcohol Dehydrogenation

Bohyeon Kim,[§] Isaac Daniel,[§] Mark Douthwaite,^{*} Samuel Pattison,^{*} Graham J. Hutchings,^{*} and Steven McIntosh^{*}



Cite This: *ACS Catal.* 2024, 14, 8488–8493



Read Online

ACCESS |

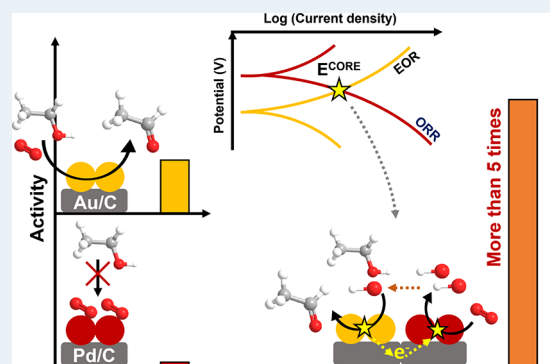
Metrics & More

Article Recommendations

Supporting Information

ABSTRACT: Cooperative redox enhancement (CORE) between physically separated but electrochemically connected catalysts promotes thermocatalytic reactions. Using the oxidative dehydrogenation of ethanol as a model reaction, we showcase two electrochemical approaches that predict monometallic and (CORE-enabled) bimetallic thermocatalytic activities. The common approach of linear sweep voltammetry can accurately determine the activity of individual half-reactions but does not account for competitive adsorption. This can lead to the underprediction of thermocatalytic rates and to overlooking the possibility of leveraging CORE effects. In contrast, adapting utilizing the Tafel method, with both reactants present, can accurately predict thermocatalytic rates and the coupling between separated catalysts.

KEYWORDS: bimetallic catalysis, redox, electron transfer, oxidative dehydrogenation, electrochemical method, rate enhancement

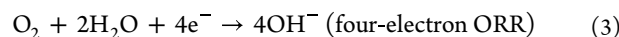
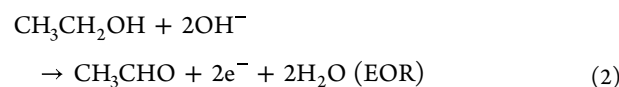
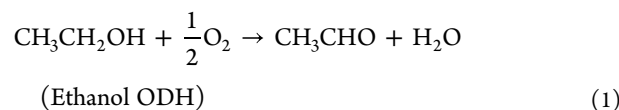


As the chemical industry shifts toward a more sustainable future, the direct integration of renewable energy sources will become increasingly important. The use of electrocatalysis in place of traditionally used heterogeneous catalysis will be crucial to this transition.^{1,2} While these two disciplines are traditionally considered to be separate, recent work has demonstrated that electrocatalytic concepts can provide important insights into the behavior of thermocatalysts.^{3–11} For example, Thejas et al.¹² presented that the OCP of the catalyst during a thermochemical reaction can provide mechanistic insights into the reaction. Their results indicate quantitatively similar trends of reaction rate and increase in OCP because of the enhancement of interfacial electrostatic effects. Yuanya et al.¹³ introduced a numerical model to predict the kinetic parameters of a thermocatalytic reaction based on electrochemical evaluations.

In prior work, we used the oxidative dehydrogenation (ODH) of 5-hydroxymethylfurfural (HMF) in alkaline media to demonstrate that electrochemical redox coupling can occur between two catalysts. The physical separation of active sites on a conductive support leads to substantial thermocatalytic rate enhancement.^{3–6} This promotional effect, termed cooperative redox enhancement (CORE), is attributed to the dissimilar activity and selectivity of the two disparate (but coupled) metals toward the half-reactions. The resulting polarization of the two catalysts via galvanic coupling drives the overall reaction at a higher rate than that which is possible on monometallic equivalents.⁶ Herein, we expand the methodologies used to study CORE, using the selective ODH of

ethanol as our model reaction. We illustrate the experimental approaches necessary to characterize the CORE phenomenon and translate electrocatalytic measurements into thermocatalytic systems, to predict thermocatalytic behavior.

Ethanol ODH can be separated into two half-reactions: the ethanol oxidation reaction (EOR) and the oxygen reduction reaction (ORR):



Acetaldehyde is highly reactive, and it can easily be oxidized to acetic acid by the following reaction.

Received: December 15, 2023

Revised: May 7, 2024

Accepted: May 14, 2024

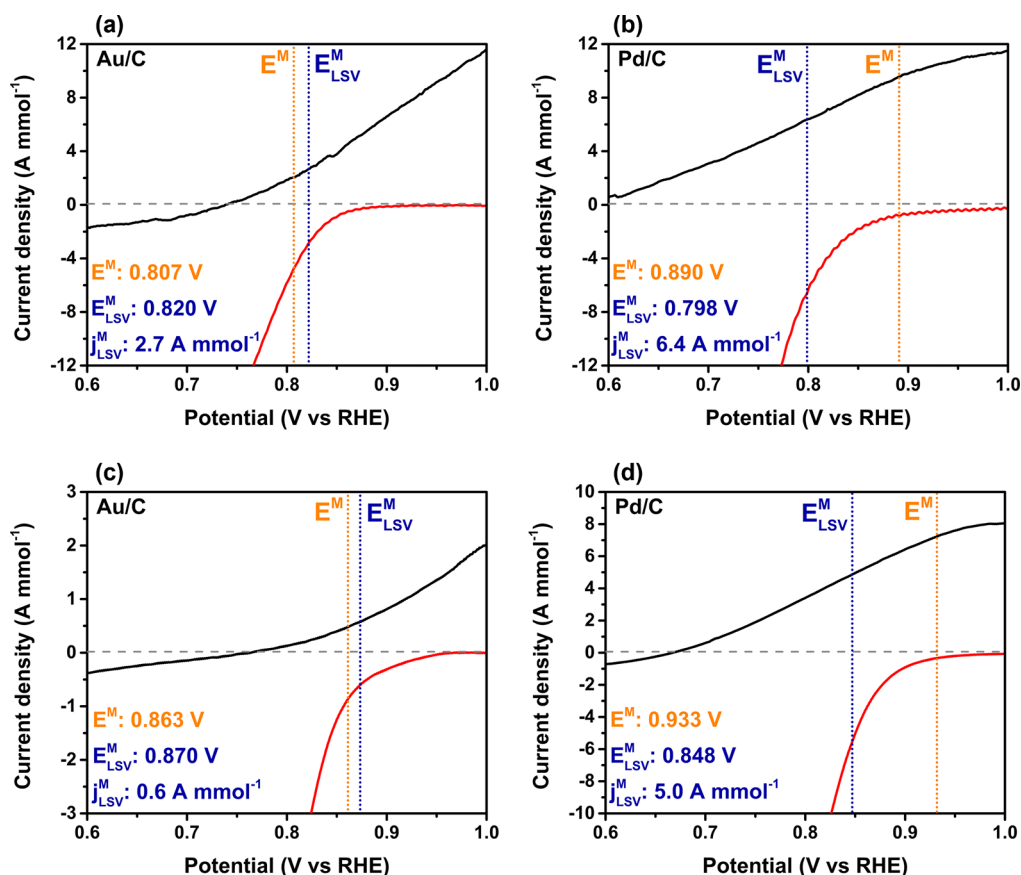
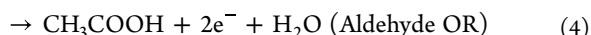
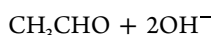


Figure 1. LSV curves of (a) Au/C and (b) Pd/C for EOR (black line) and ORR (red line) at 50 °C. The same experiments were conducted at RT with (c) Au/C and (d) Pd/C. The values of E_{LSV}^M and j_{LSV}^M are shown in the figure indicated as navy color. E^M was measured from an independent experiment but present in the same place for comparison. Reaction conditions (EOR, black line): 0.8 M ethanol, 1.6 M Na_2CO_3 , 50 mL min^{-1} of nitrogen. Reaction conditions (ORR, red line): 1.6 M Na_2CO_3 , 50 mL min^{-1} of oxygen, Reaction conditions (E^M): 0.8 M ethanol, 1.6 M Na_2CO_3 , 50 mL min^{-1} of oxygen. Note that the E^M for Au/C and Pd/C is above the O_2 diffusion-limited potential range determined for our electrodes, Figure S2.



For continuity with our previous work,^{3–6} we utilize a Au/C and Pd/C catalytic couple in this system. Physically separated Au and Pd nanoparticles on Vulcan carbon were synthesized following the same procedure in our prior publications.^{5,6} As we have previously shown, the Au and Pd remain as separated nanoparticles and do not form an alloys under experimental conditions.^{5,6} Au/C is a well-established catalyst for the thermocatalytic reaction, and both electrocatalytic half-reactions.^{14–17} In contrast, despite the fact that the EOR and ORR electrocatalytic activity of Pd/C has been demonstrated,^{18–21} the thermocatalytic oxidation of ethanol over Pd appears to have been overlooked.

Based on mixed potential theory, the observed potential is realized when the rate of anodic and cathodic reactions are balanced, which is widely accepted in a corrosion-type reaction.^{22–24} The catalytic activity of each half-reaction can be independently characterized electrochemically via the current density and converted into a molar rate using Faraday's law. Simple thermochemical aerobic oxidations on mono-metallic or alloy catalysts have been evaluated by these electrochemical approaches revealing reasonable predictions.^{7–9,25} Furthermore, CORE operates through galvanic coupling, a well-known electrochemical phenomenon.^{8,22,23,26}

Thus, it was considered logical to draw from this body of literature to develop methods of accurately interpreting thermocatalytic systems using electrocatalytic approaches.

It is relatively straightforward to measure the mixed potential, E^M , for individual catalysts with both ethanol and oxygen present, Figure S1a. With no applied electrochemical driving force, this potential is equivalent to that which occurs during an analogous thermocatalytic reaction. This is the OCP at which the rates of electron generation and consumption by the EOR and the ORR, respectively, are balanced through an effective electrical short-circuit through the conductive support. The electrocatalytic rates of each half-reaction can be independently measured by exposing the catalyst to only one reactant and performing linear sweep voltammetry (LSV), Figure S1b. From this, it is then possible to predict a mixed potential where the anodic and cathodic reactions are balanced, denoted as E_{LSV}^M with corresponding current density j_{LSV}^M , Figure S1b. If the two reactants interact with the catalyst surface completely independently and both are present with no other kinetic barriers, the two mixed potentials should be the same, i.e., E_{LSV}^M should equal E^M .

This is the approach previously leveraged by Ryu et al.⁷ to interpret aerobic oxidation over single or alloy catalysts and has provided a basis for how we can interpret the CORE mechanism.⁶ Despite the excellent agreement of the approach in the previous reports, combining independent half-reaction

measurements cannot always predict the performance in the mixed reactant system. We illustrate this by examining Au/C and Pd/C for ethanol ODH, Figure 1.

Over Au/C, there is good consistency with the idealized theory at both 50 °C and room temperature (RT), Figure 1a and 1c. The individual LSV curves for the EOR and ORR indicate that Au/C is active for both half-reactions, aligning with studies reporting that Au-based catalysts exhibit high thermocatalytic activity for the ODH of ethanol.^{15,17} When combined, the predicted mixed potential, E_{LSV}^M , is within experimental reproducibility of the mixed potential from OCP measurements, E^M . The mixed current density, j_{LSV}^M , at 50 °C can be converted to an equivalent thermocatalytic rate of 0.6×10^{-7} mol s⁻¹. Considering the conditional differences and loss of active surface area upon incorporating nanoparticles onto an electrode, it shows a remarkable correlation with the ODH activity, $1.23 \pm 0.232 \times 10^{-7}$ mol s⁻¹. Evidently, in this example, the LSV approach is robust and facilitates the quantification of the thermocatalytic activity.

In contrast, over the Pd/C, Figure 1b, the values for E_{LSV}^M and E^M do not align (0.798 V vs 0.890 V, respectively), with LSV predicting a thermocatalytic reaction rate of 1.33×10^{-7} mol s⁻¹ at 50 °C, 19 times higher than the observed thermocatalytic rate of $0.077 \pm 0.232 \times 10^{-7}$ mol s⁻¹. It is worth noting that the E^M is far closer to the ORR onset potential of 0.910 V (at 0.5 A mmol⁻¹), which suggests that surface-adsorbed oxygen may block sites and inhibit interactions between ethanol and Pd, when both reactants are present. The poor prediction of the thermocatalytic activity from the j_{LSV}^M is rationalized by the disagreement of E_{LSV}^M and E^M . The lack of alignment between the mixed potentials for Pd/C suggests that the two-half reactions do not occur on independent catalytic sites and that competitive adsorption may be a factor. Two sets of step change measurements, Figure S3 and Figure S4, were conducted for both catalysts. For Au/C, the equilibration to the same potential, irrespective of the direction of approach, suggests that both oxygen and ethanol actively interact simultaneously with the Au/C surface. In the case of Pd/C, after the injection of oxygen, the rise in potential above the E_{LSV}^M and toward the ORR onset potential suggests the displacement of adsorbed ethanol by oxygen, which is in agreement with several studies.^{20,27,28} Additionally, competitive adsorption on Pd, and respective alloys, in the presence of oxygen has been extensively studied in fuel cell catalysis.^{29–31} It is well established that even small proportions of Pd species can inhibit the influence of ethanol that can be crossed over from the anodic side, achieving excellent ORR stability in the ethanol fuel cell.³²

A H-Cell was utilized at 50 °C to determine the EOR products of Au/C and Pd/C when holding the anode at the E^M determined from Figure 1. Acetic acid was formed with a faradaic efficiency of 89.9% for Au/C and 96.4% for Pd/C. Similar results were obtained from thermochemical tests, Figure S7. This indicates the primary oxidation route on Au/C and Pd/C for both thermo- and electrochemical tests is through acetaldehyde and its further oxidation to acetic acid. Note that the E^M of Pd/C is higher than the onset potential of Pd oxide further indicating that cycling of Pd between Pd⁰ and Pd²⁺ is likely a key step in the catalytic cycle.³ XPS analysis of these catalysts,⁶ confirmed the existence of Pd²⁺ in pre- and postreaction catalysts. It should also be noted that a small amount of acetaldehyde is likely lost during these experiments to its low boiling point of 20.2 °C.

Tafel plot analysis is a possible alternative approach to measure overall reaction rates, Figure S5.^{33,34} Crucially, the measurement is conducted in the presence of both the reductant and oxidant, accounting for the competitive adsorption behavior of reactants. Herein, we denote the obtained Tafel potential as E_{Tafel}^M and Tafel current density as j_{Tafel}^M by Tafel extrapolation, Figure 2 and Figure S6. While

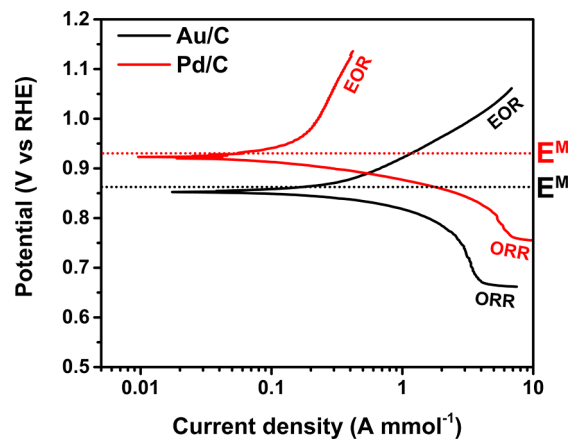


Figure 2. Tafel slopes of (a) Au/C and Pd/C. The dotted black and red lines indicate the E^M of Au/C and Pd/C, respectively. Reaction conditions (Tafel, E^M): 0.8 M ethanol, 1.6 M Na₂CO₃, 50 mL min⁻¹ of oxygen, RT.

these experiments were conducted at room temperature to simplify the experimental system, as shown in Figure 1 and our prior work,⁶ room temperature experiments are excellent predictors for the elevated temperature activity and presence of the CORE phenomenon.

Given that these measurements are acquired in the same chemical environment, the E_{Tafel}^M are in near-perfect agreement with the previously determined E^M for both catalysts. Examining the EOR branch of both Tafel plots, Au/C demonstrates a substantially higher EOR rate in the presence of oxygen (3.51 A mmol⁻¹ at 1.0 V) than Pd/C (0.23 A mmol⁻¹ at 1.0 V) in agreement with the trend in measured thermocatalytic activities for the overall reaction. Crucially, Tafel analysis accounts for the oxygen inhibition, which influences the EOR rate. This is effectively illustrated by the lower Tafel current density and high Tafel slope for the EOR branch of the Pd/C Tafel curve and indicates that there is a lower thermocatalytic rate for ethanol ODH on Pd/C than on Au/C. It is however important to note that the LSV approach remains valid when competitive factors are not rate-limiting, or when one wishes to determine the activities of the individual half-cell reactions alone.

In our previously reported description of CORE effects,⁶ the separation of the anodic and cathodic half reactions between catalysts and the polarization of both active sites form a new mixed potential, denoted as E^{CORE} , which is measured as an open circuit potential of the mixed catalyst with both reactants present. The cathodic polarization of one metal and the anodic polarization of the other accelerate the overall thermocatalytic rate. This coupling is analogous to active galvanic corrosion, where the corrosion rate (anodic oxidation reaction) of one metal is accelerated by electrochemical polarization when coupled to a dissimilar metal performing the cathodic ORR.^{35–37} In CORE, the anodic corrosion reaction is replaced with a selective electrochemical oxidation, previously demon-

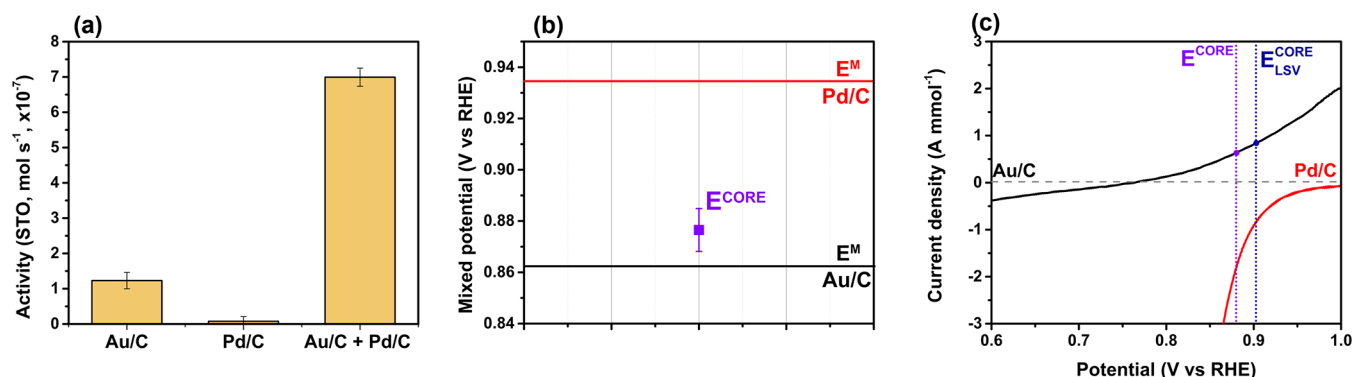


Figure 3. (a) Activity of ODH of ethanol on Au/C, Pd/C, and Au/C + Pd/C after 30 min. (b) Comparison of E^M of Au/C and Pd/C and its mixture Au/C + Pd/C, E^{CORE} , obtained from the OCP measurements. (c) LSV curves of Au/C (black line, HMFOR) and Pd/C (red line, ORR). Reaction conditions of the thermocatalytic reaction: 0.8 M ethanol, 1.6 M Na₂CO₃, 3 bar of oxygen, 60 °C. Reaction conditions of the OCP measurements: 0.8 M ethanol, 1.6 M Na₂CO₃, 50 mL min⁻¹ of oxygen, RT. The reaction conditions of Figure 3c are given in Figure 1.

strated with the HMF dehydrogenation (DH) and herein with the ethanol DH.⁶

Such corrosion couples are typically analyzed via a Tafel plot, as in Figure 2. The crossover in Pd/C ORR and Au/C EOR Tafel curves is directly analogous to the crossover expected for active galvanic corrosion of dissimilar metals, hence predicting that we will observe CORE effect in this case. Considering the thermocatalytic data, Figure 3a, the ethanol ODH rate observed for the physically mixed Au/C + Pd/C catalyst is 5.35 times higher than the direct summation of the rates observed on Au/C and Pd/C, with the same total metal loading, Figure 3a. As discussed above, the overall rate of Pd/C is very low due to the high oxygen coverage on the surface, however, Pd/C is active for the ORR. Measuring the CORE potential of the Au/C + Pd/C catalyst system yields an E^{CORE} of 0.877 ± 0.01 V, Figure 3b, which lies between the E^M values of the individual catalysts, as predicted by the crossover point in the Tafel plots, Figure 2. This confirms that through coupling, both catalytic sites are polarized, enhancing the rate of each half-reaction.

By combining the LSV curves for the ORR on Pd/C and EOR on Au/C, we can examine an idealized scenario where the ORR occurs exclusively on Pd/C and the EOR exclusively on Au/C, Figure 3c. Determining the potential of equal cathodic and anodic current density yields an LSV-predicted CORE potential, E_{LSV}^{CORE} , of 0.902 V at a current density of 0.85 A mmol⁻¹. Alternatively, the E^{CORE} determined by OCP measurement, 0.877 V, yields a slightly lower current density of 0.63 A mmol⁻¹. The CORE potential and current density from LSV tests and OCP measurements are, as expected, close to the crossover point in the Tafel plots, 0.889 V and 0.536 A mmol⁻¹, Figure 2.

The slight differences in E^{CORE} values among the Tafel, LSV, and OCP approaches are reasonable considering that the complete separation of the half-reactions assumed from the LSV method is not feasible in actual thermocatalytic reactions. While we can predict that there will be a significant separation between half-reactions using electrochemical measurements, the thermocatalytic system is far more complex. In the Au/C + Pd/C thermocatalytic system, we must expect incomplete separation due to the random nature of the catalyst particle distribution. Despite this, we have demonstrated that the active, CORE-derived, spontaneous polarization of the two metals separates the half-reactions to a significant extent, accelerating both half-reactions, and leading to a greater than

5-fold increase in the observed thermocatalytic reaction rate. In the case discussed herein, we leverage CORE to enable the high ORR activity of Pd/C without requiring the EOR to occur on this oxygen-dominated surface. Half-reaction separation due to CORE can circumvent limitations of competitive adsorption that otherwise limit the overall rates on monometallic catalysts.

In summary, we have described the advantages of utilizing the Tafel approach to predict thermocatalytic reaction rates. The LSV method, designed to capture individual half-cell reaction activities in an isolated electrochemical cell, is clearly limited when competitive adsorption between reactants plays a significant role in limiting the reaction rate. Tafel measurements are conducted in the presence of both reactants and thus more accurately reflect the thermocatalytic reaction conditions. Thus, while LSV is useful to understand the rates of individual half-reactions, the Tafel approach is necessary to fully translate this to the thermocatalytic rates for both monometallic and CORE-enabled bimetallic catalysts. The Tafel method can predict the presence of CORE between Au/C and Pd/C, and demonstrate that this enhanced rate is due to the separation of half-reactions between electrochemically coupled physically separated catalysts.

■ ASSOCIATED CONTENT

Supporting Information

The Supporting Information is available free of charge at <https://pubs.acs.org/doi/10.1021/acscatal.3c06103>.

Schematics explaining the electrochemical experimental setup. Electrochemical analysis for monitoring the adsorption trends of the catalysts. Thermochemical activity and carbon balance data. Materials and methods for electrochemical and thermochemical analysis, and catalyst synthesis. Supplementary references (PDF)

■ AUTHOR INFORMATION

Corresponding Authors

Steven McIntosh – Department of Chemical and Biomolecular Engineering, Lehigh University, Bethlehem, Pennsylvania 18015, United States; orcid.org/0000-0003-4664-2028; Email: stm310@lehigh.edu

Mark Douthwaite – Max Planck-Cardiff Centre on the Fundamentals of Heterogeneous Catalysis FUNCAT, Cardiff Catalysis Institute, School of Chemistry, Cardiff University,

Translational Research Hub, Cardiff CF24 4HQ, U.K.;
Email: douthwaitejm@cardiff.ac.uk

Graham J. Hutchings – Max Planck-Cardiff Centre on the
Fundamentals of Heterogeneous Catalysis FUNCAT, Cardiff
Catalysis Institute, School of Chemistry, Cardiff University,
Translational Research Hub, Cardiff CF24 4HQ, U.K.;
orcid.org/0000-0001-8885-1560; Email: hutch@
cardiff.ac.uk

Authors

Bohyeon Kim – Department of Chemical and Biomolecular
Engineering, Lehigh University, Bethlehem, Pennsylvania
18015, United States

Isaac Daniel – Max Planck-Cardiff Centre on the
Fundamentals of Heterogeneous Catalysis FUNCAT, Cardiff
Catalysis Institute, School of Chemistry, Cardiff University,
Translational Research Hub, Cardiff CF24 4HQ, U.K.

Samuel Patisson – Max Planck-Cardiff Centre on the
Fundamentals of Heterogeneous Catalysis FUNCAT, Cardiff
Catalysis Institute, School of Chemistry, Cardiff University,
Translational Research Hub, Cardiff CF24 4HQ, U.K.

Complete contact information is available at:
<https://pubs.acs.org/10.1021/acscatal.3c06103>

Author Contributions

[§]B.K. and I.T.D. contributed equally. B.K., I.T.D., M.D., S.P., G.J.H., and S.M. conceived and conceptualized the project. B.K. and I.T.D. conducted the experimental investigation and performed the data analysis. M.D., S.P., G.J.H., and S.M. provided project supervision. G.J.H. and S.M. provided funding acquisition. The manuscript was finalized and edited through the contributions of all authors. All authors have given approval to the final version of the manuscript.

Funding

S.M. and B.K. would like to thank Lehigh University for its financial support. I.T.D., M.D., S.P., and G.J.H. would like to thank the Max Planck Centre on the Fundamentals of Heterogeneous Catalysis (FUNCAT) for funding.

Notes

The authors declare no competing financial interest.

ACKNOWLEDGMENTS

We would like to thank Kylie Park for her helpful input and discussion.

REFERENCES

- (1) Möhle, S.; Zirbes, M.; Rodrigo, E.; Gieshoff, T.; Wiebe, A.; Waldvogel, S. R. Modern Electrochemical Aspects for the Synthesis of Value-Added Organic Products. *Angew. Chemie - Int. Ed.* **2018**, *57* (21), 6018–6041.
- (2) Suen, N. T.; Hung, S. F.; Quan, Q.; Zhang, N.; Xu, Y. J.; Chen, H. M. Electrocatalysis for the Oxygen Evolution Reaction: Recent Development and Future Perspectives. *Chem. Soc. Rev.* **2017**, *46* (2), 337–365.
- (3) Huang, X.; Akdim, O.; Douthwaite, M.; Wang, K.; Zhao, L.; Lewis, R. J.; Patisson, S.; Daniel, I. T.; Miedziak, P. J.; Shaw, G.; Morgan, D. J.; Althabhan, S. M.; Davies, T. E.; He, Q.; Wang, F.; Fu, J.; Bethell, D.; McIntosh, S.; Kiely, C. J.; Hutchings, G. J. Au–Pd Separation Enhances Bimetallic Catalysis of Alcohol Oxidation. *Nature* **2022**, *603* (7900), 271–275.
- (4) Zhao, L.; Akdim, O.; Huang, X.; Wang, K.; Douthwaite, M.; Patisson, S.; Lewis, R. J.; Lin, R.; Yao, B.; Morgan, D. J.; Shaw, G.; He, Q.; Bethell, D.; McIntosh, S.; Kiely, C. J.; Hutchings, G. J. Insights into the Effect of Metal Ratio on Cooperative Redox

Enhancement Effects over Au- and Pd-Mediated Alcohol Oxidation. *ACS Catal.* **2023**, *13* (5), 2892–2903.

(5) Daniel, I. T.; Zhao, L.; Bethell, D.; Douthwaite, M.; Patisson, S.; Lewis, R. J.; Akdim, O.; Morgan, D. J.; McIntosh, S.; Hutchings, G. J. Kinetic Analysis to Describe Co-Operative Redox Enhancement Effects Exhibited by Bimetallic Au–Pd Systems in Aerobic Oxidation. *Catal. Sci. Technol.* **2023**, *13* (1), 47–55.

(6) Daniel, I. T.; Kim, B.; Douthwaite, M.; Patisson, S.; Lewis, R. J.; Cline, J.; Morgan, D. J.; Bethell, D.; Kiely, C. J.; McIntosh, S.; Hutchings, G. J. Electrochemical Polarization of Disparate Catalytic Sites Drives Thermochemical Rate Enhancement. *ACS Catal.* **2023**, *13* (21), 14189–14198.

(7) Ryu, J.; Bregante, D. T.; Howland, W. C.; Bisbey, R. P.; Kaminsky, C. J.; Surendranath, Y. Thermochemical Aerobic Oxidation Catalysis in Water Can Be Analysed as Two Coupled Electrochemical Half-Reactions. *Nat. Catal.* **2021**, *4* (9), 742–752.

(8) Fortunato, G. V.; Pizzutilo, E.; Katsounaros, I.; Göhl, D.; Lewis, R. J.; Mayrhofer, K. J. J.; Hutchings, G. J.; Freakley, S. J.; Ledendecker, M. Analysing the Relationship between the Fields of Thermo- and Electrocatalysis Taking Hydrogen Peroxide as a Case Study. *Nat. Commun.* **2022**, *13* (1), 1–7.

(9) Adams, J. S.; Kromer, M. L.; Rodríguez-López, J.; Flaherty, D. W. Unifying Concepts in Electro- And Thermocatalysis toward Hydrogen Peroxide Production. *J. Am. Chem. Soc.* **2021**, *143* (21), 7940–7957.

(10) An, H.; Sun, G.; Hülsey, M. J.; Sautet, P.; Yan, N. Demonstrating the Electron-Proton-Transfer Mechanism of Aqueous Phase 4-Nitrophenol Hydrogenation Using Unbiased Electrochemical Cells. *ACS Catal.* **2022**, *12* (24), 15021–15027.

(11) Howland, W. C.; Gerken, J. B.; Stahl, S. S.; Surendranath, Y. Thermal Hydroquinone Oxidation on Co/N-Doped Carbon Proceeds by a Band-Mediated Electrochemical Mechanism. *J. Am. Chem. Soc.* **2022**, *144* (25), 11253–11262.

(12) Wesley, T. S.; Román-Leshkov, Y.; Surendranath, Y. Spontaneous Electric Fields Play a Key Role in Thermochemical Catalysis at Metal-Liquid Interfaces. *ACS Cent. Sci.* **2021**, *7* (6), 1045–1055.

(13) Zhao, Y.; Adams, J. S.; Baby, A.; Kromer, M. L.; Flaherty, D. W.; Rodríguez-López, J. Electrochemical Screening of Au/Pt Catalysts for the Thermocatalytic Synthesis of Hydrogen Peroxide Based on Their Oxygen Reduction and Hydrogen Oxidation Activities Probed via Voltammetric Scanning Electrochemical Microscopy. *ACS Sustain. Chem. Eng.* **2022**, *10* (51), 17207–17220.

(14) Beyhan, S.; Uosaki, K.; Felii, J. M.; Herrero, E. Electrochemical and in Situ FTIR Studies of Ethanol Adsorption and Oxidation on Gold Single Crystal Electrodes in Alkaline Media. *J. Electroanal. Chem.* **2013**, *707*, 89–94.

(15) Varela, H.; de Lima, R. B. Catalytic Oxidation of Ethanol on Gold Electrode in Alkaline Media. *Gold Bull.* **2008**, *41* (1), 15–22.

(16) Cao, X.; Li, C.; Peng, D.; Lu, Y.; Huang, K.; Wu, J.; Zhao, C.; Huang, Y. Highly Strained Au Nanoparticles for Improved Electrocatalysis of Ethanol Oxidation Reaction. *J. Phys. Chem. Lett.* **2020**, *11* (8), 3005–3013.

(17) Zope, B. N.; Hibbitts, D. D.; Neurock, M.; Davis, R. J. Reactivity of the Gold/Water Interface during Selective Oxidation Catalysis. *Science* (80-). **2010**, *330* (6000), 74–78.

(18) Liang, Z. X.; Zhao, T. S.; Xu, J. B.; Zhu, L. D. Mechanism Study of the Ethanol Oxidation Reaction on Palladium in Alkaline Media. *Electrochim. Acta* **2009**, *54* (8), 2203–2208.

(19) Guo, J.; Chen, R.; Zhu, F.-C.; Sun, S.-G.; Villullas, H. M. New Understandings of Ethanol Oxidation Reaction Mechanism on Pd/C and Pd2Ru/C Catalysts in Alkaline Direct Ethanol Fuel Cells. *Appl. Catal. B Environ.* **2018**, *224*, 602–611.

(20) Jiang, L.; Hsu, A.; Chu, D.; Chen, R. Oxygen Reduction Reaction on Carbon Supported Pt and Pd in Alkaline Solutions. *J. Electrochem. Soc.* **2009**, *156* (3), B370.

(21) Fu, G.; Wu, K.; Lin, J.; Tang, Y.; Chen, Y.; Zhou, Y.; Lu, T. One-Pot Water-Based Synthesis of Pt-Pd Alloy Nanoflowers and Their Superior Electrocatalytic Activity for the Oxygen Reduction

Reaction and Remarkable Methanol-Tolerant Ability in Acid Media. *J. Phys. Chem. C* **2013**, *117* (19), 9826–9834.

(22) Power, G.P.; Ritchie, I.M. Mixed Potential Measurements in the Elucidation of Corrosion Mechanisms-I. Introductory Theory. *Electrochim. Acta* **1981**, *26* (8), 1073–1078.

(23) Power, G. P.; Staunton, W. P.; Ritchie, I. M. Mixed Potential Measurements in the Elucidation of Corrosion Mechanisms-II. Some Measurements. *Electrochim. Acta* **1982**, *27* (1), 165–169.

(24) Bindra, P.; Light, D.; Rath, D. Mechanisms of Electroless Metal Plating: I. Mixed Potential Theory and the Interdependence of Partial Reactions. *J. Appl. Electrochem.* **1984**, *28* (6), 668–678.

(25) Mallat, T.; Baiker, A. Catalyst Potential Measurement: A Valuable Tool for Understanding and Controlling Liquid Phase Redox Reactions. *Top. Catal.* **1999**, *8*, 115–124.

(26) Plowman, B. J.; O'Mullane, A. P.; Bhargava, S. K. The Active Site Behaviour of Electrochemically Synthesised Gold Nanomaterials. *Faraday Discuss.* **2011**, *152*, 43.

(27) Yin, S.; Cai, M.; Wang, C.; Shen, P. K. Tungsten Carbide Promoted Pd-Fe as Alcohol-Tolerant Electrocatalysts for Oxygen Reduction Reactions. *Energy Environ. Sci.* **2011**, *4* (2), 558–563.

(28) Rao, C. V.; Viswanathan, B. Carbon Supported Pd-Co-Mo Alloy as an Alternative to Pt for Oxygen Reduction in Direct Ethanol Fuel Cells. *Electrochim. Acta* **2010**, *55* (8), 3002–3007.

(29) Yang, J.; Lee, J. Y.; Zhang, Q.; Zhou, W.; Liu, Z. Carbon-Supported Pseudo-Core–Shell Pd–Pt Nanoparticles for ORR with and without Methanol. *J. Electrochem. Soc.* **2008**, *155* (7), B776–B781.

(30) Li, H.; Sun, G.; Jiang, Q.; Zhu, M.; Sun, S.; Xin, Q. Preparation and Characterization of Pd/C Catalyst Obtained in NH₃-Mediated Polyol Process. *J. Power Sources* **2007**, *172* (2), 641–649.

(31) Li, X.; Huang, Q.; Zou, Z.; Xia, B.; Yang, H. Low Temperature Preparation of Carbon-Supported Pd-Co Alloy Electrocatalysts for Methanol-Tolerant Oxygen Reduction Reaction. *Electrochim. Acta* **2008**, *53* (22), 6662–6667.

(32) Antolini, E. Palladium in Fuel Cell Catalysis. *Energy Environ. Sci.* **2009**, *2* (9), 915–931.

(33) McCafferty, E. Validation of Corrosion Rates Measured by the Tafel Extrapolation Method. *Corros. Sci.* **2005**, *47* (12), 3202–3215.

(34) Shi, Z.; Liu, M.; Atrens, A. Measurement of the Corrosion Rate of Magnesium Alloys Using Tafel Extrapolation. *Corros. Sci.* **2010**, *52* (2), 579–588.

(35) Mansfeld, F.; Hengstenberg, D. H.; Kenkel, J. V. Galvanic Corrosion of Al Alloys I. Effect of Dissimilar Metal. *Corrosion* **1974**, *30* (10), 343–353.

(36) Mansfeld, F.; Kenkel, J. V. Galvanic Corrosion of Al Alloys - II. Effect of Solution Composition. *Corros. Sci.* **1975**, *15* (3), 183–198.

(37) Society, E. E.; Bode, H.; Brodd, T. R. J.; Kordesch, K. V. *Uhlig's Corrosion Handbook*; John Wiley & Sons, Inc., 2011. DOI: 10.1002/9780470872864.